Comparative Methods for Estimating Parameters of the Generalized Pareto Distribution with Application to Extreme Rainfall in Bangkok

AUTCHA ARAVEEPORN[1,*], PARADORN SUKPAN[1], KANCHANA KUMNUNGKIT[2]
[1]Department of Statistics, School of Science,
King Mongkut's Institute of Technology Ladkrabang
10520, Bangkok,
THAILAND

[2]Department of Mathematics, School of Science,
King Mongkut's Institute of Technology Ladkrabang
10520, Bangkok,
THAILAND

*Corresponding Author

Abstract: - This study aims to compare the performance of various parameter estimation methods for the Generalized Pareto Distribution (GPD) in modeling and forecasting the return level of yearly maximum rainfall in Bangkok, Thailand. Four estimation methods, namely Maximum Likelihood (ML), Generalized Maximum Likelihood (GML), Bayesian, and L-Moments, were investigated through both simulation experiments and real data analyses. In the simulation study, data were generated with fixed location and scale parameters, varying shape parameters, and threshold percentiles. The results indicated that the ML method performed best for short-tailed distributions, the GML method for medium-tailed distributions, and the L-Moments method for heavy-tailed distributions. Using 360 monthly observations (January 1994–December 2023) from four rainfall stations, including QSNCC, Don Mueang, Bang Na, and Klong Toey, the GPD model was fitted to the real data. The results revealed that the L-Moments method achieved the lowest Root Mean Square Error (RMSE) across all stations, confirming its superior performance in estimating extreme rainfall. The return level analysis for return periods of 2-9 years showed an increasing trend in extreme rainfall at all stations. Overall, the study concludes that the L-Moments-based GPD model is the most effective method for fitting extreme rain in Bangkok.

Key-Words: - Bayesian Estimation, Extreme Rainfall, Extreme Value Theory, Generalized Pareto Distribution, L-Moments, Parameter Estimation, Peak Over Threshold, Return Level.

Received: February 5, 2026. Revised: April 9, 2026. Accepted: August 2, 2026. Published: September 17, 2026.

1 Introduction

The Extreme Value Theorem (EVT) provides a conceptual and methodological framework for modeling random variables that describe extreme events, such as maxima and minima. Foundational studies by [1] and [2] established the Generalized Pareto Distribution (GPD) as a model to characterize tail behavior in probability distributions. Although extreme observations are often excluded in standard analyses due to their complexity, they are essential for understanding the probability of rare events such as heavy rainfall, high wind speeds, or temperature extremes. EVT has been widely applied in hydrology [3], flood risk assessment [4], and climate change analysis [5], with recent methodological improvements proposed by [6] to enhance parameter estimation accuracy.

The Peak Over Threshold (POT) approach is particularly well-suited for applications involving a large number of observations, such as high-frequency daily data. A suitable threshold is selected, and all exceedances beyond this value are analyzed using the Generalized Pareto Distribution (GPD), first introduced by [7]. Further developments by h [8] enhanced inference methods and threshold selection for POT modeling. To reduce temporal dependence among exceedances, a delustering technique is often applied, [9]. However, no declustering procedure was applied in the present study because the analysis was based on monthly maximum rainfall rather than daily threshold exceedances. Within EVT, two essential measures, the return level and return period, describe the magnitude and frequency of extreme events, estimated from historical data. The POT and GPD concepts have been widely applied in coastal engineering [10], and climate studies [11], offering a practical probabilistic approach to assess future extreme events.

The GPD is a three-parameter probability distribution with location, scale, and shape parameters. Depending on the value of the shape parameter, the GPD encompasses characteristics of tailed behavior, corresponding to the exponential distribution.

Parameter estimation plays a crucial role in EVA, particularly for GPD, for which several techniques have been developed. Among them, the Maximum Likelihood (ML) method is the commonly used approach in statistics. The fundamental principle of ML estimation is to determine the parameter values that maximize the likelihood function, thereby identifying the parameters that make the observed data most probable. The Generalized Maximum Likelihood Estimation (GML) method extends the traditional ML approach and is particularly advantageous when the likelihood function is complex or analytically intractable. Another necessary approach is Bayesian estimation, which combines the prior distribution with the observed data to obtain the posterior distribution. Additionally, the L-moments method offers an alternative approach to parameter estimation by summarizing the characteristics of the probability distribution in a manner that is less sensitive to outliers and sampling variability.

Several studies have contributed to improving and applying these estimation techniques. The study by [12] investigated GPD parameters estimated using the ML method. Monte Carlo simulations confirmed that ML provides efficient and consistent estimates, with variances decreasing as sample size increases. The authors in [13] introduced new Bayesian methods for estimating GPD parameters, a key model in EVT. Traditional approaches, such as ML and Probability-Weighted Moments, use only data exceeding a certain threshold, resulting in information loss. To overcome this limitation, the authors proposed two novel Bayesian methods that incorporate the complete information contained in the baseline distribution and leverage the functional dependencies between the baseline and GPD parameters.

L-moments and Generalized Maximum Likelihood (GML) estimation provide robust frameworks for modeling economic variables with heavy-tailed distributions such as GPD growth and extreme macroeconomic events. The works of [14] and [15] demonstrated that L-moments are particularly suitable for analyzing economic data characterized by high variability and non-normality, offering more stable and unbiased estimates than traditional moment-based methods. Meanwhile, studies [16] and [17] established the theoretical foundation for GML estimation in extreme value modeling, emphasizing its efficiency and flexibility in handling nonstationary behavior. Integrating these approaches enables the development of a unified framework for comparing MLE, GML, Bayesian, and L-moments methods in parameter estimation, thereby enhancing the accuracy and interpretability of models applied to GPD dynamics and extreme economic fluctuations.

Bangkok, the capital city of Thailand, is located on the lower floodplain of the Chao Phraya River. The city has undergone rapid urban and economic expansion, yet it continues to experience recurrent flooding that severely impacts livelihoods, transportation, and infrastructure. The leading causes include its low-lying topography, insufficient drainage systems, and the impacts of climate change. Heavy rainfall between May and October frequently leads to extensive waterlogging in many urban areas.

To accurately assess the risk of extreme rainfall in Bangkok, this case employs EVT, specifically the GPD, to model exceedances of rainfall thresholds and estimate the probability of severe flood events. The GPD employs a fitting-parameter technique to analyze the frequency and magnitude of extreme events, providing valuable insights for flood risk management, infrastructure planning, and sustainable urban development.

Research based on EVT that emphasizes the GPD has been widely conducted across rainfall volumes. For instance, the study in [18] applied the GPD to analyze extreme rainfall events in Thailand’s Chi watershed, using daily data from 1984 to 2022.

Results identified Udon Thani, Chaiyaphum, Maha Sarakham, Roi Et, and Sisaket as high-risk areas with the highest return levels for continuous rainfall events. The developed return level maps support effective flood prediction and management, emphasizing the importance of incorporating extreme rainfall analysis into sustainable water resource planning under climate change. The method proposed in [19] developed an automatic and statistically robust method for selecting optimal thresholds in extreme rainfall analysis, utilizing the

Generalized Pareto and Pareto–Poisson distributions by integrating weighted least squares estimation, studentized residuals, and independence testing. Validation with numerical experiments and NOAA–GHCN rainfall data shows superior accuracy and stability compared to traditional approaches.

Collectively, these studies emphasize that accurate parameter estimation, through Maximum Likelihood (ML), Generalized Maximum Likelihood (GML), Bayesian, or L-moments methods, is fundamental for reliable modeling of extreme events based on the GPD. Such precision in estimating GPD parameters enables a better understanding, prediction, and management of rare but high-impact occurrences.

2 Parameter Estimation Methods

The GPD is specifically designed for modeling observations that exceed a predetermined threshold. Within EVT, it forms the basis of the Peaks-Over-Threshold (POT) approach, which models exceedances above a sufficiently high threshold.

Let u denote a predetermined threshold, and let:

$$Y = X - u \mid X > u,$$

represent the exceedances over the threshold. Under the POT framework, the exceedance variable Y follows a GPD distribution with scale parameter $\sigma > 0$ and shape parameter ξ. Equivalently, the original variable X may be represented by a three-parameter GPD with location parameter $\mu = u$. Since the threshold is predetermined before parameter estimation, the location parameter remains fixed throughout this study, and only the scale and shape parameters are estimated using the Maximum Likelihood (ML), Generalized Maximum Likelihood (GML), Bayesian, and L-moments methods.

The Cumulative Distribution Function (CDF) of the GPD is given by

$$F(x;\mu,\sigma,\xi) = \begin{cases} 1 - \left[1 + \xi\left(\dfrac{x-\mu}{\sigma}\right)\right]^{-\frac{1}{\xi}}, & \xi \neq 0 \\ 1 - \exp\left(-\dfrac{x-\mu}{\sigma}\right), & \xi = 0, \end{cases} \tag{1}$$

where $\sigma > 0$, $1 + \xi\left(\dfrac{x-\mu}{\sigma}\right) > 0.$

The corresponding probability density function of the GPD is expressed as:

$$f(x;\mu,\sigma,\xi) = \begin{cases} \dfrac{1}{\sigma}\left[1 + \xi\left(\dfrac{x-\mu}{\sigma}\right)\right]^{-1+\frac{1}{\xi}}, & \xi \neq 0 \\ \dfrac{1}{\sigma}\exp\left(-\dfrac{x-\mu}{\sigma}\right), & \xi = 0. \end{cases} \tag{2}$$

The mean and variance of the GPD are derived as"

$$E(X) = \mu + \frac{\sigma}{1-\xi}, \quad \xi < 1$$

and $Var(X) = \dfrac{\sigma^2}{(1-2\xi)(1-\xi)^2}, \quad \xi < \dfrac{1}{2}.$

The GPD can be classified into three distinct types, depending on the value of the shape parameter ξ: $\xi = 0$ the distribution exhibits a medium-tailed behavior, corresponding to the exponential distribution, $\xi > 0$ the distribution has a heavy tail, characteristic of Pareto-type behavior, and $\xi < 0$ the distribution displays a short-tail, indicating a bounded upper limit. Parameter estimation is a fundamental statistical procedure for determining the values of parameters in probability distributions or statistical models.

2.1 Maximum Likelihood (ML)

The ML is the most widely used statistical method for estimating parameters of probability distributions. It is favored due to its conceptual simplicity, sound theoretical foundation, and desirable asymptotic properties. The main idea of ML is to find parameter values that maximize the likelihood function, which represents the joint probability of the observed data given the parameters.

Parameter estimation for the GPD involves constructing and maximizing the likelihood function to obtain the model parameters. The procedure begins by defining the probability density function that characterizes the likelihood of observing a particular sample from the distribution. The assumption of the data follow a GPD from (2), the likelihood function can be expressed as

$$L(\mu,\sigma,\xi) = \frac{1}{\sigma^k}\prod_{i=1}^{k}\left[\left(1 + \xi\left(\frac{x_i-\mu}{\sigma}\right)\right)^{-\left(1+\frac{1}{\xi}\right)}\right], \tag{3}$$

where μ, σ, and ξ denote the location, scale, and shape parameters, respectively, and k represents the number of exceedances above a specified threshold. For computational convenience, the log-likelihood function is determined by taking the logarithm of the likelihood function from (3), resulting in

$$l(\mu,\sigma,\xi) = -k\log(\sigma) - \left(1+\frac{1}{\xi}\right)\sum_{i=1}^{k}\log\left[1+\xi\left(\frac{x_i-\mu}{\sigma}\right)\right]. \quad (4)$$

The parameter estimation is obtained by differentiating the log-likelihood function in (4) with respect to each parameter (σ,ξ) and equating the partial derivatives to zero, thereby yielding the system of equations used to calculate the maximum likelihood estimators. The location parameter (μ) remains fixed because it is determined by the selected percentile threshold. Since these likelihood equations are nonlinear and typically lack closed-form analytical solutions, numerical optimization algorithms are employed. In this study, the Newton–Raphson iterative method [20], [21] was used to efficiently solve the likelihood equations and obtain stable, accurate estimates of the GPD parameters. Initial parameter values were obtained from preliminary estimates, and the iterative procedure continued until the maximum absolute change in the parameter estimates was less than 10^{-6}. The optimization was performed under the constraint $\sigma > 0$, and alternative starting values were used whenever numerical instability or nonconvergence occurred.

2.2 Generalized Maximum Likelihood (GML)

The GML method, initially proposed by [22], extends classical ML by allowing the incorporation of prior information or non-parametric elements into the estimation process. It is especially useful when the likelihood equations cannot be solved analytically or when the assumptions of ML are overly restrictive. The GML approach, also known as the generalized likelihood estimator, enhances the likelihood function by incorporating supplementary information, thereby improving both the accuracy and stability of the parameter estimates.

In the context of the GPD, the GML approach was refined by [23], who introduced a prior density function for the shape parameter ξ to reflect the uncertainty and prior knowledge about its range. The prior distribution of ξ is modeled using a Beta distribution, defined as:

$$\pi(\xi) = \frac{(0.5+\xi)^{u-1}(0.5-\xi)^{v-1}}{B(u,v)}, -0.5 \le \xi \le 0.5, u=6, v=9,$$

where $B(u,v) = \frac{\Gamma(u)\Gamma(v)}{\Gamma(u+v)}$ is the Beta function, with an expected value $E(\xi) = -0.1$ and variance $Var(\xi) = 0.015$. This prior constrains the shape parameter within a realistic range, enhancing numerical stability and reducing bias in small samples.

The Generalized Likelihood Function (GLF) for the GPD is then defined as the traditional likelihood and the prior density function, as follows:

$$GL(\mu,\sigma,\xi) = L(\mu,\sigma,\xi)\,\pi(\xi), \quad (5)$$

where $L(X;\mu,\sigma,\xi)$ is the standard likelihood function of the GPD, expressed as

$$GL(\mu,\sigma,\xi) = \frac{1}{\sigma^k}\prod_{i=1}^{k}\left[\left(1+\xi\left(\frac{x_i-\mu}{\sigma}\right)\right)^{-\left(1+\frac{1}{\xi}\right)}\right]\pi(\xi) \quad (6)$$

for $\xi \neq 0$ and k representing the number of exceedances above the threshold. Taking the logarithm of Equation (6) yields the generalized log-likelihood function,

$$l_G(\mu,\sigma,\xi) = -k\log(\sigma) - \left(1+\frac{1}{\xi}\right)\sum_{i=1}^{k}\log\left[1+\xi\left(\frac{x_i-\mu}{\sigma}\right)\right] + \log\{\pi(\xi)\}. \quad (7)$$

The parameter estimates $\hat{\sigma}$ and $\hat{\xi}$ are given by maximizing the generalized log-likelihood function with respect to the parameters. The location parameter remains fixed at the selected threshold as the ML. This involves solving the system of partial derivative equations:

$$\frac{\partial l_G(\mu,\sigma,\xi)}{\partial\sigma} = 0 \text{ and } \frac{\partial l_G(\mu,\sigma,\xi)}{\partial\xi} = 0.$$

Since these equations are highly nonlinear and lack closed-form analytical solutions, numerical optimization algorithms are employed. The Newton–Raphson iterative method is commonly used to solve the likelihood equations and locate the parameter values that maximize the generalized log-likelihood function. This iterative approach continues until the change in parameter estimates between successive iterations falls below a predefined tolerance, ensuring convergence to the optimal estimates.

2.3 Bayesian Method

The Bayesian approach provides a probabilistic framework for parameter estimation by combining prior information with data.

In the Bayesian paradigm [24], parameters $\theta = (\mu, \sigma, \xi)$ are treated as random variables with prior distributions. Given the observed data $x = (x_1, x_2, ..., x_n)$ the likelihood function based on the GPD is exhibited in equation (3). The posterior distribution, which combines both the prior information and the observed data, is derived via Bayes' theorem as:

$$\pi(\theta | x) = \frac{L(\theta | x)\pi(\theta)}{\int L(\theta | x)\pi(\theta)d\theta},$$

where $\pi(\theta)$ defines the prior and $\pi(\theta | x)$ denotes the posterior distribution of the parameters given the observed data.

The selection of prior distributions is a crucial step in Bayesian inference. The weakly informative priors can be employed to avoid implausible values while maintaining flexibility, such as:

$\sigma \sim \text{Inverse-Gamma}(0.1, 0.1)$, $\xi \sim \text{Normal}(0, 10^2)$, and $\mu \sim \text{Uniform}(\min(x), \max(x))$.

Because the posterior distribution lacks a closed-form expression, simulation-based algorithms such as Markov Chain Monte Carlo (MCMC) [25], [26] are typically employed. Commonly used methods include the Metropolis–Hastings algorithm, [27]. A typical MCMC algorithm proceeds as follows:

1) Initialize $\theta^{(0)} = (\mu^{(0)}, \sigma^{(0)}, \xi^{(0)})$.
2) Generate candidate parameters θ^* from a multivariate normal random-walk proposal distribution $q(\theta^* | \theta(t-1))$.
3) Compute the acceptance ratio:
$$r = \min\left(1, \frac{L(\theta^* | x)\pi(\theta^*)q(\theta^{(t-1)} | \theta^*)}{L(\theta^{(t-1)} | x)\pi(\theta^{(t-1)})\, q(\theta^* | \theta^{(t-1)})}\right).$$
4) Accept the new state with probability r; otherwise, retain the previous value.
5) Repeat Steps 2–4 for 20,000 iterations. The first 5,000 iterations were discarded as the burn-in period. Thereafter, every 5th sample was retained to reduce autocorrelation, yielding 3,000 posterior samples for inference. Posterior means were used as point estimates of the model parameters, and posterior standard deviations, along with 95% credible intervals, were computed from the retained samples.

The resulting chain of posterior samples $\{\theta^{(t)}\}_{t=1}^{T}$ is used to estimate posterior means, standard deviations, and credible intervals. T denotes the number of retained posterior samples after discarding the burn-in iterations and applying thinning as $T = 3{,}000$. Bayesian estimation was implemented in R using the extRemes package.

Once a sufficiently large number of MCMC samples is obtained, parameter estimates and credible intervals are computed as:

$$\hat{\theta}_{Bayes} = \frac{1}{T}\sum_{t=1}^{T}\theta^{(t)}.$$

2.4 L-moments Method

The L-moments are summary statistics that are linear functions of the order statistics. They provide robust and nearly unbiased measures of threshold fixed value, scale, and shape, and are less sensitive to sampling variability and outliers than conventional moments.

For a random variable X with the distribution function $f(x)$, the r-th population L-moment [28] is defined as:

$$\lambda_r = \frac{1}{r}\sum_{k=0}^{r-1}(-1)^k \binom{r-1}{k} E\left[X_{(r-k:r)}\right],\ r = 1, 2, ... \quad (8)$$

where $X_{(r-k;r)}$ denotes the $(r-k)$-th order statistic from a sample of size r .The first four L-moments can be interpreted analogously to conventional moments: λ_1 denotes L-mean (location) and λ_2 denotes L-scale. The dimensionless ratios:

$$\tau_3 = \frac{\lambda_3}{\lambda_2} \text{ and } \tau_4 = \frac{\lambda_4}{\lambda_2}$$

represent L-skewness and L-kurtosis, respectively.

For the GPD, the theoretical L-moments can be expressed in closed form [29]. The first two population L-moments, for $\xi < 1$ are:

$$\lambda_1 = \mu + \frac{\sigma}{1-\xi},\ \lambda_2 = \frac{\sigma}{(1-\xi)(2-\xi)}.$$

The population L-skewness is:

$$\tau_3 = \frac{\lambda_3}{\lambda_2} = \frac{1+\xi}{3-\xi}.$$

Let $y_1, y_2, ..., y_n$ denote the threshold exceedances, where $y_i = x_i - u$, and let $y_{(1)} \le y_{(2)} \le ... y_{(n)}$ denote the corresponding ordered observations. The sample probability-weighted moments [30] are calculated as

$$b_r = \frac{1}{n}\sum_{i=r+1}^{n} \frac{\binom{i-1}{r}}{\binom{n-1}{r}} y_{(i)}, \; r = 0,1,2,... \tag{9}$$

The first three sample L-moments are then obtained from $\ell_1 = b_0,\ \ell_2 = 2b_1 - b_0$, and $\ell_3 = 6b_2 - 6b_1 + b_0$.

The sample L-skewness is defined as $t_3 = \dfrac{\ell_3}{\ell_2}$.

By equating the theoretical and sample L-moment ratios, the L-moment estimator of the shape parameter is:

$$\hat{\xi} = \frac{3t_3 - 1}{1 + t_3}.$$

The corresponding scale parameter estimator is:

$$\hat{\sigma} = \ell_2(1-\hat{\xi})(2-\hat{\xi}).$$

Because the location parameter corresponds to the predetermined POT threshold, it is fixed as $\mu = u$, and is not estimated separately. Therefore, in this study, the L-moments method is used to estimate only the scale and shape parameters. Unlike the likelihood-based methods, these estimators are available in explicit form and do not require numerical optimization.

3 Simulation Study

The simulation focused on moderate-to-large exceedance samples to investigate the asymptotic behavior of the estimators. The use of relatively large sample sizes is justified because rainfall observations are collected as time-series data over extended periods. Larger samples better preserve the temporal characteristics and variability of extreme rainfall events, thereby providing more stable and efficient parameter estimates. In this study, four sample sizes (300, 500, 700, and 1000) were considered, and each simulation was repeated 1,000 times. Nevertheless, future studies should also investigate smaller exceedance samples (e.g., 30–100 observations), which are more commonly encountered in practical POT applications. The simulated data were generated from the GPD with the location parameter (μ) set to 2, the scale parameter (σ) set to 2, and the shape parameter (ξ) taking values of −0.3, 0, and 0.3, respectively, as illustrated in Figure 1.

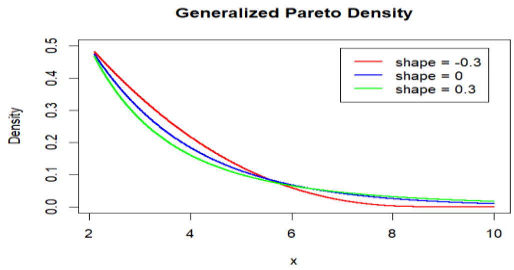

Fig. 1: Probability density functions of the GPD under different shape parameter values (ξ=-0.3, 0, 0.3).

Source: created by the authors.

Thresholds corresponding to the 85th, 90th, and 95th percentiles were initially evaluated. The 90th percentile was selected for parameter estimation because it yielded the lowest mean squared error (MSE) among the candidate thresholds. The GPD parameters were approximated using four methods: ML, GML, Bayesian, and L-moments. The performance of these estimation methods was evaluated and compared based on the Mean Squared Error (MSE) criterion, with the method yielding the lowest MSE considered the most efficient and reliable for parameter estimation. The MSE is a measure used to assess the accuracy of estimates based on the magnitude of prediction errors. It is susceptible to large deviations because each error term is squared before averaging. The MSE can be computed using Equation (9):

$$MSE = \frac{1}{m}\sum_{i=1}^{m}\left(\theta - \hat{\theta}_i\right)^2, \tag{10}$$

where θ_i denotes the true parameter value obtained from the GPD distribution with $\theta = (\sigma, \xi)$, $\hat{\theta}_i$ represents the estimated parameter obtained from the simulation of the GPD distribution $\theta_i = (\sigma_i, \xi_i)$, and m is the number of simulation replications generated from the GPD distribution. The mean of the estimated parameter is computed as:

$$\bar{\theta} = \frac{\sum_{i=1}^{m}\hat{\theta}_i}{m}.$$

A lower MSE value indicates that the estimated parameters are closer to the actual parameters, implying higher estimation model reliability. After the parameter estimation, the results are presented in Table 1, Table 2 (Appendix) and Table 3.

Table 1. The mean and MSE for the parameter estimation in the case of $\mu = 2, \sigma = 2, \xi = -0.3$.

n	Methods	Parameter Scale (σ)	Parameter Shape (ξ)	MSE Scale (σ)	MSE Shape (ξ)
300	ML	1.1315	-0.4244	0.8524	0.0661
	GML	0.9207	-0.2153	1.2189	0.0344
	Bayesian	1.0303	-0.2120	1.0173	0.0719
	L-Moments	1.0094	-0.2980	1.0638	0.0616
500	ML	1.0687	-0.3713	0.9145	0.0279
	GML	0.8975	-0.2021	1.2433	0.0259
	Bayesian	1.0117	-0.2569	1.0174	0.0269
	L-Moments	1.0007	-0.2977	1.0451	0.0356
700	ML	1.0499	-0.3464	0.9344	0.0165
	GML	0.9141	-0.2133	1.2051	0.0215
	Bayesian	1.0099	-0.2680	1.0092	*0.0162*
	L-Moments	1.0017	-0.2922	1.0342	0.0269
1,000	ML	1.0362	-0.3326	0.9482	0.0097
	GML	0.9235	-0.2247	1.1772	0.0161
	Bayesian	1.0073	-0.2786	1.0033	0.0093
	L-Moments	1.0010	-0.2930	1.0224	0.0183

Source: created by the authors.

From Table 1, the mean and MSE of the location parameter remain constant for all sample sizes (n = 300, 500, 700, 1000) and across all estimation techniques, with mean values of 5.3008, 5.3130, 5.3211, and 5.3198, and corresponding MSE values of 10.9267, 10.9936, 11.0434, and 11.0305, respectively. For the shape parameter, L-moments show mean estimates that approach the true parameter values as the sample size increases, indicating consistency of the estimators. Regarding MSE performance, the ML method yields the lowest MSE for the scale parameter across nearly all sample sizes, demonstrating its efficiency in estimating the scale parameter under this scenario. In contrast, for the shape parameter, the GML and Bayesian methods provide the smallest MSE values, particularly at larger sample sizes, reflecting their superior accuracy. Overall, the results confirm that increasing the sample size improves estimation accuracy for all methods, with ML performing best for the scale parameter and GML/Bayesian showing strong performance for the shape parameter. The MSE illustrates the comparison of these parameter estimates in Figure 2.

Figure 2 illustrates the MSE trends for the scale and shape parameters under different estimation methods. For the scale parameter, the MSE decreases consistently across all methods except for the ML estimator, whose MSE shows a slight upward trend as the sample size increases. In contrast, for the shape parameter, all estimation methods show a clear decline in MSE as sample size increases, indicating improved estimation accuracy. These patterns confirm that larger sample sizes enhance estimator performance, particularly for the scale and shape parameters in the GML, Bayesian, and L-moments methods.

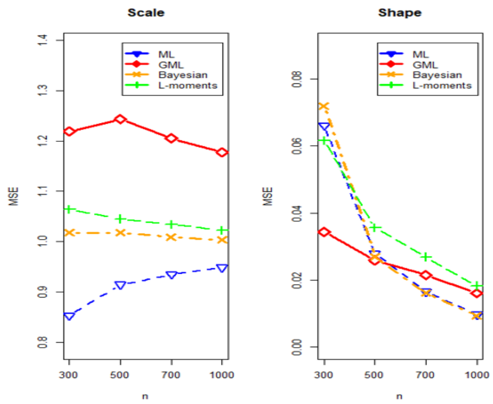

Fig. 2: The plots of the MSE of the scale and shape parameters estimated by setting $\mu = 2, \sigma = 2, \xi = 0$.

Source: created by the authors.

From Table 2 (Appendix), the mean and MSE of the location parameter remain constant for all sample sizes and estimation methods, with mean values of 6.5700, 6.5956, 6.5901, and 6.6011, and corresponding MSE values of 20.9926, 21.1873, 21.1178, and 21.2049, respectively. This indicates that the location parameter is stably estimated regardless of sample size or method. For the scale and shape parameters, the L-moments method shows mean values that approach the true parameter values as the sample size increases, confirming the consistency of the estimators. In terms of MSE performance, the GML method provides the lowest MSE for both the scale and shape parameters across all sample sizes. The MSE illustrates the comparison of these parameter estimates in Figure 3.

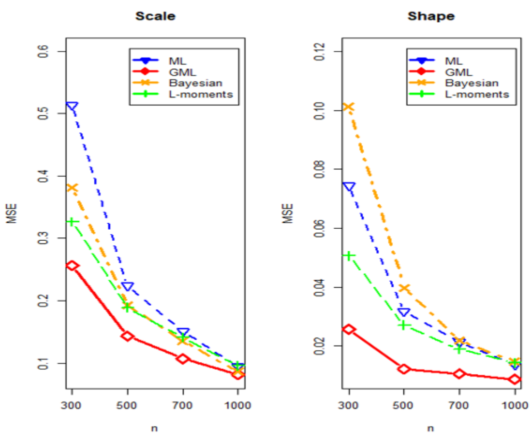

Fig. 3: The plots of the MSE of the scale and shape parameters estimated by setting $\mu = 2$, $\sigma = 2, \xi = 0$.

Source: created by the authors.

Figure 3 illustrates the MSE trends for the scale and shape parameters across the four estimation methods as the sample size increases. For both the scale and shape parameters, the MSE decreases consistently across all estimation techniques when the sample size increases, indicating improved estimation accuracy and greater stability of the methods with larger data sets.

Table 3. The mean and MSE for parameter estimation in the case of $\mu = 2, \sigma = 2, \xi = 0.3$.

n	Methods	Parameter		MSE	
		Scale (σ)	Shape (ξ)	Scale (σ)	Shape (ξ)
300	ML	4.4263	0.2074	7.9954	0.0832
	GML	5.0360	0.0930	11.8936	0.1110
	Bayesian	4.2156	0.4683	6.7860	0.1327
	L-Moments	4.1456	0.2410	6.0560	0.0460
500	ML	4.2354	0.2475	6.0230	0.0397
	GML	4.7991	0.1403	9.5607	0.0810
	Bayesian	4.1028	0.3921	5.3797	0.0537
	L-Moments	4.0902	0.2644	5.2140	0.0275
700	ML	4.1152	0.2623	5.1500	0.0262
	GML	4.5437	0.1751	7.6750	0.0586
	Bayesian	4.0328	0.3589	4.7948	0.0312
	L-Moments	4.0278	0.2712	4.7284	0.0202
1,000	ML	4.0578	0.2777	4.6673	0.0178
	GML	4.3178	0.2213	6.1012	0.0384
	Bayesian	4.0093	0.3405	4.4629	0.0200
	L-Moments	3.9970	0.2827	4.3812	0.0143

Source: created by the authors.

The mean and MSE of the location parameter remain constant for all sample sizes and estimation approaches, with mean estimates of 8.6293, 8.6267, 8.6067, and 8.6371 and corresponding MSE values of 44.4196, 44.2003, 43.8581, and 44.1978, respectively. This stability indicates that the location parameter is not affected by the estimation procedure used in this study. For the shape parameter, the L-moments method yields estimates that are consistently closest to the true value across all sample sizes. In terms of estimation accuracy, the L-moments method also produces the lowest MSE values for both the scale and shape parameters, demonstrating superior robustness and performance. As the sample size increases, the MSE decreases across all methods, further confirming the consistency of the estimators, as shown in Figure 4.

Figure 4 shows that for both the scale and shape parameters, the MSE decreases consistently across all estimation methods when the sample size becomes larger. This indicates that the accuracy and stability of parameter estimation improve systematically with increasing sample size for every method considered.

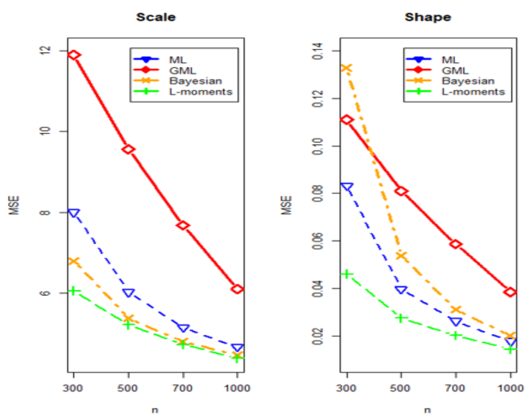

Fig. 4: The plots of the MSE of the scale and shape parameters estimated by setting $\mu = 2$, $\sigma = 2, \xi = 0.3$.

Source: created by the authors.

The location parameter remains constant across all sample sizes and estimation methods because it is fixed at the predetermined threshold corresponding to the 90th percentile of the data. In the POT–GPD framework, the location parameter represents the threshold and is therefore not estimated. Likewise, in the simulation study, the location parameter is specified as a known constant, while all estimation methods, including ML, GML, Bayesian, and L-moments, are used to estimate only the scale and shape parameters. Consequently, the location parameter remains unchanged throughout the analysis, resulting in identical mean and MSE values across all estimation methods and sample sizes.

4 Application on Actual Data

The rainfall data used in this study are secondary data obtained from the Thai Meteorological Department. The dataset consists of monthly maximum rainfall records collected from January 1994 to December 2023, totaling 360 months, across four meteorological stations: Queen Sirikit National Convention Center (QSNCC), Don Mueang, Bang Na, and Klong Toey, as illustrated in Figure 5, Figure 6, Figure 7 and Figure 8.

Although POT is commonly applied to daily rainfall exceedances, daily rainfall observations from all four stations were not consistently available over the entire study period. Therefore, the monthly maximum rainfall was used to create a homogeneous dataset spanning 30 years. For the monthly maximum rainfall data obtained from the four meteorological stations in Bangkok, the descriptive statistics, including the mean, standard deviation, coefficient of skewness, coefficient of kurtosis, minimum, and maximum values, are summarized in Table 4.

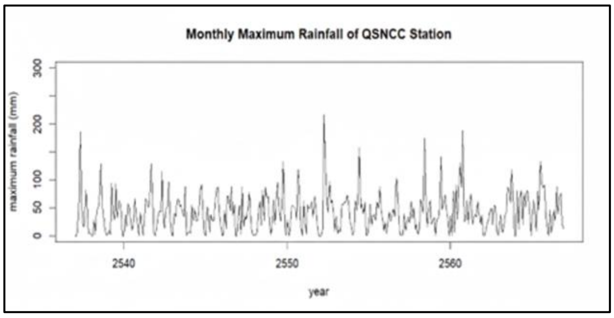

Fig. 5: Monthly maximum rainfall at the Queen Sirikit National Convention Center (QSNCC) station.
Source: created by the authors.

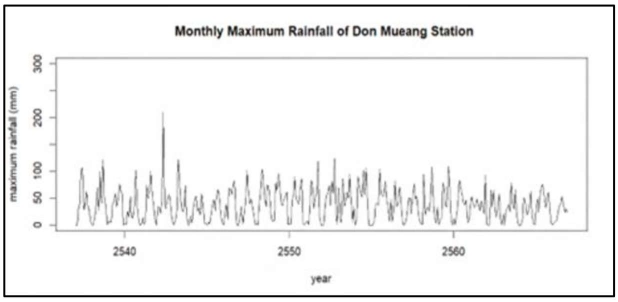

Fig. 6: Monthly maximum rainfall at the Don Mueang station.
Source: created by the authors.

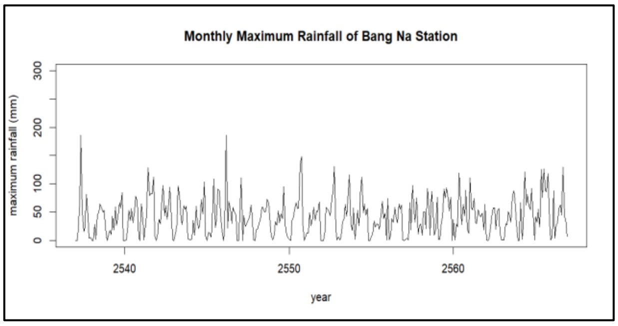

Fig. 7: Monthly maximum rainfall at the Bang Na station.
Source: created by the authors.

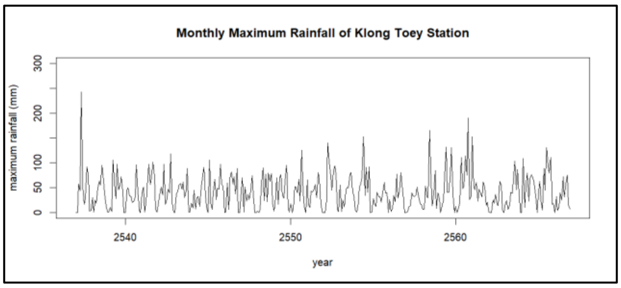

Fig. 8: Monthly maximum rainfall at the Klong Toey station.
Source: created by the authors.

Table 4. Descriptive statistics of monthly maximum rainfall at each meteorological station

Statistic	QSNCC	Don Mueang	Bang Na	Klong Toey
Minimum	0.0	0.0	0.0	0.0
Maximum	216.8	210.7	185.9	242.6
Mean	41.5964	36.7911	41.5675	41.1825
Standard Deviation	34.6669	30.8009	33.6561	35.3754
Skewness	1.3679	1.0355	0.9628	1.3651
Kurtosis	6.3097	5.1659	4.3538	6.4617

Source: created by the authors.

As shown in Table 4, the Klong Toey station recorded the highest monthly maximum rainfall among all stations. It exhibited the most significant standard deviation, indicating considerable variability in monthly rainfall extremes. When considering the overall monthly maximum rainfall data, the Queen Sirikit National Convention Center (QNSCC) station showed the highest mean value of 41.5964 mm. The coefficients of skewness for all stations are positive, indicating that the monthly maximum rainfall data are right-skewed. Likewise, the kurtosis coefficients for all stations are greater than zero, indicating that the rainfall distributions are more peaked and have heavier tails than the normal distribution. Histograms illustrating these distributional characteristics are shown in Figure 9.

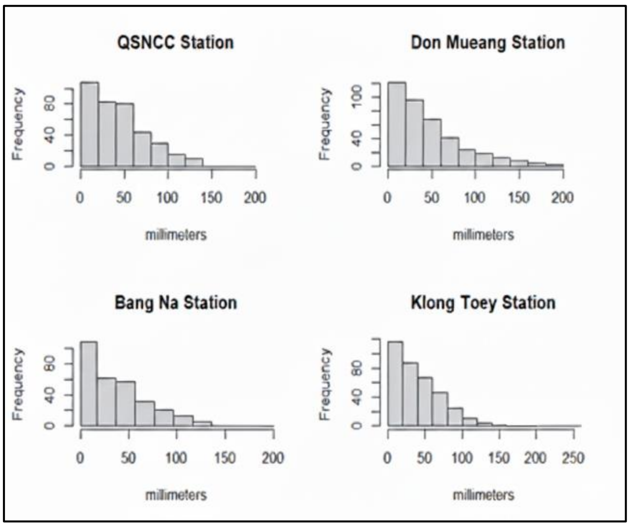

Fig. 9: Histograms of monthly maximum rainfall at four rainfall stations in Bangkok: QSNCC, Don Mueang, Bang Na, and Klong Toey.
Source: created by the authors.

For parameter estimation, the monthly maximum rainfall was modeled using the GPD, with a POT threshold set at the 90th percentile to characterize extreme rainfall events. This approach focuses on modeling exceedances above a selected threshold to effectively characterize extreme rainfall behavior. The results of the POT analysis, including the scale and shape values, are summarized in Table 5, Table 6, Table 7 and Table 8.

Table 5. Estimated parameters of the monthly maximum rainfall data at the QSNCC station.

Methods	Parameters	
	Scale (σ)	Shape (ξ)
ML	24.3124	0.1819
GML	33.0217	-0.0811
Bayesian	23.3567	0.4715
L-Moments	22.3069	0.2436

Source: created by the authors.

Table 6. Estimated parameters of the monthly maximum rainfall data at the Don Mueang station.

Methods	Parameters	
	Scale (σ)	Shape (ξ)
ML	25.4354	0.0000
GML	25.4241	-0.0719
Bayesian	20.2701	0.3960
L-Moments	24.8935	-0.0904

Source: created by the authors.

Table 7. Estimated parameters of the monthly maximum rainfall data at the Bang Na station

Methods	Parameters	
	Scale (σ)	Shape (ξ)
ML	28.0224	0.0214
GML	32.0992	-0.1027
Bayesian	24.1178	0.4654
L-Moments	23.8367	0.1664

Source: created by the authors.

Table 8. Estimated parameters of the monthly maximum rainfall data at the Klong Toey station

Methods	Parameters	
	Scale (σ)	Shape (ξ)
ML	21.7432	0.1504
GML	27.7883	-0.0437
Bayesian	22.3065	0.3821
L-Moments	24.4936	0.0481

Source: created by the authors.

According to Table 5, Table 6, Table 7 and Table 8, the threshold (location parameter) remained fixed across the four rainfall stations because it was predetermined as the 90th percentile of the observed rainfall data. The corresponding threshold values were 81.77 for the QSNCC station, 82.05 for the Don Mueang station, 81.41 for the Bang Na station, and 82.26 for the Klong Toey station. These threshold values represent the station-specific reference levels above which rainfall exceedances were modeled using the Generalized Pareto Distribution (GPD). Since the threshold was fixed prior to parameter estimation, only the scale and shape parameters were estimated in the POT–GPD analysis.

The GPD-based forecasting models were estimated using station-specific parameters, which were used to compute return levels for return periods of 2, 3, 4, …, and 10 years.

For the GPD with parameters σ and ξ, when considering the exceedances over a specified threshold u, the probability that a random variable $X > u$ can be expressed as

$$P(X > u) = \zeta_u \left(1+\xi\left(\frac{x-u}{\sigma}\right)\right)^{-1/\xi}, \qquad (11)$$

where $\zeta_u = P(X > u)$. The return level represents the quantile associated with an average exceedance once every T years. For any given threshold u, the corresponding return period T is defined by:

$$\zeta_u \left(1+\xi\left(\frac{x-u}{\sigma}\right)\right)^{-1/\xi} = \frac{1}{T}. \qquad (12)$$

The return level for the GPD model can therefore be estimated as:

$$\hat{x}_T^{GDP} = \hat{\mu} - \frac{\hat{\sigma}}{\hat{\xi}}\left[\left(T\zeta_u\right)^{\xi} - 1\right], \qquad (13)$$

where n_x denotes the number of observations per year, and N represents the total number of years. Hence, the return period T is given by $T = N \times n_x$.

The adequacy and estimation performance of each model were evaluated using the Root Mean Square Error (RMSE), which quantifies the prediction accuracy of each estimation method. A smaller RMSE indicates that the estimated return levels are closer to the observed monthly maximum rainfall, implying better predictive performance. The calculation of the RMSE can be expressed as:

$$RMSE = \sqrt{\frac{1}{9}\sum_{T=1}^{9}(x_T - \hat{x}_T^{GPD})^2},$$

where x_T denotes the observed value at a given return period T and $\hat{x}_T^{GPD}$ represents the estimated return level at the corresponding return period T. The results are summarized in Table 9.

Table 9. The lowest RMSE value corresponds to the annual series of monthly maximum rainfall data

Methods	Stations			
	QSNCC	Don Mueang	Bang Na	Klong Toey
ML	58.60	57.34	37.26	48.89
GML	57.86	53.82	37.79	49.20
Bayesian	75.72	68.65	48.81	55.97
L-Moments	58.50	52.11	36.92	49.31

Source: created by the authors.

Among the four stations listed in Table 9, Bang Na Station consistently exhibits the smallest RMSE values across all estimation methods, indicating the highest estimation accuracy. When comparing estimation techniques, the L-Moments method generally yields the most accurate results, with the lowest RMSE values across most stations, as shown in Figure 10, followed closely by the GML method. These findings suggest that the L-Moments method is more efficient and stable for estimating return levels of extreme rainfall.

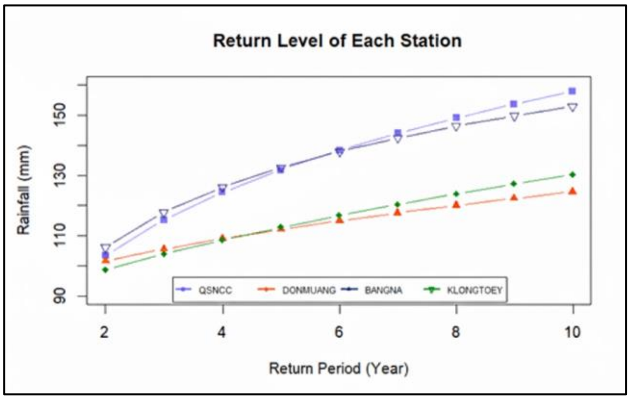

Fig. 10: Return level plots of the annual series of monthly maximum rainfall for each rainfall observation station by the L-moments method. *Source: created by the authors.*

After identifying the most appropriate model and estimation method for the maximum monthly rainfall data at Bang Na station, the model adequacy was further assessed using diagnostic plots, including the Probability–Probability (PP) Plot, Quantile–Quantile (QQ) Plot, and Probability Density Plot, as illustrated in Figure 11. These graphical evaluations provide comprehensive validation of the model's fit and the suitability of the selected distribution for estimating extreme rainfall.

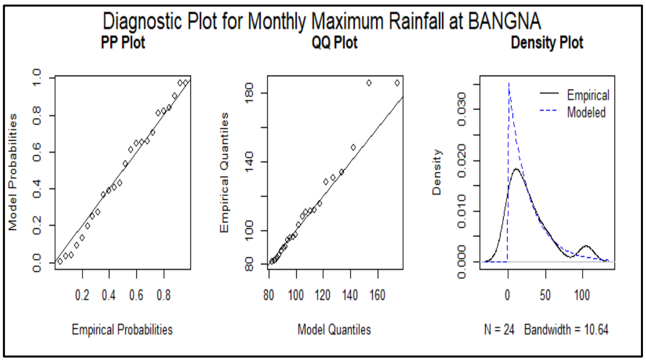

Fig. 11: Diagnostic plots for the fitted model of monthly maximum rainfall at Bang Na station. *Source: created by the authors.*

Figure 11 presents the diagnostic plots for the monthly maximum rainfall at the Bang Na Station. The PP and QQ plots demonstrate that most data points closely follow the 45-degree reference line, indicating good agreement between the empirical and modeled probabilities and quantiles. This suggests that the selected distribution adequately represents the observed rainfall extremes. Furthermore, the probability density plot shows that the modeled density closely aligns with the empirical density curve, capturing both the central tendency and tail behavior of the data. Overall, these diagnostic results confirm that the fitted model provides a satisfactory representation of the monthly maximum rainfall distribution at the Bang Na Station.

5 Conclusion

This study investigated the estimation and forecasting performance of using different estimation techniques, Maximum Likelihood (ML), Generalized Maximum Likelihood (GML), Bayesian, and L-Moments, for modeling monthly maximum rainfall in Bangkok. Simulation experiments were first conducted by setting the location and scale parameters and varying the shape parameter, while also adjusting the threshold to 90 percentiles. The results revealed that the ML method provided the lowest MSE for negative shape parameters (short-tailed distributions), the GML method performed best for zero shape parameters (medium-tailed distributions), and the L-Moments method yielded the lowest MSE for positive shape parameters (heavy-tailed distributions). For empirical analysis, monthly maximum rainfall data from four meteorological stations in Bangkok, covering a period of 360 months (January 1994 to December 2023), were analyzed. The results confirmed that the GPD model is appropriate for modeling extreme rainfall data across all stations. Among the estimation methods, the L-Moments method demonstrated the best overall performance, yielding the lowest RMSE values for all stations, indicating its robustness and superior accuracy in modeling monthly maximum rainfall extremes.

Return level analysis for return periods of 2, 3, …, 10 years showed a consistent upward trend in extreme rainfall levels across all stations. Notably, the QSNCC and Bang Na stations exhibited a sharp and nearly identical increase in return levels over time, while the Don Mueang and Klong Toey stations showed moderate but steady gains. Among all stations, Bang Na Station provided the most realistic and reliable estimation of return levels, closely matching the observed data. It is important to note that this analysis was based on 30 years of rainfall records, which may limit the precision of parameter estimation and return levels due to external and uncontrollable factors. Nevertheless, the findings emphasize the practical applicability of the L-Moments-based GPD model as a reliable tool for estimating extreme rainfall.

Future research should consider extending the length and diversity of rainfall records used for analysis. Incorporating additional data sources, such as satellite-based rainfall estimates, radar measurements, or merged gridded datasets, may improve the stability of parameter estimates and the accuracy of return-level forecasts. Moreover, developing non-stationary GPD models that incorporate covariates such as temperature trends, climate indices (e.g., ENSO), urbanization intensity, or land-use changes would provide deeper insights into how extreme rainfall patterns evolve under changing climatic and environmental conditions. Comparative studies involving Bayesian estimation, GML, or machine-learning-assisted extreme value models are also recommended. Such approaches could offer improved uncertainty quantification, enhanced flexibility, and better predictive performance, particularly in complex urban settings.

References:

[1] S. Coles, *An Introduction to Statistical Modeling of Extreme Values*, Springer, London, 2001. ISBN: 978-1-85233-459-8.

[2] P. Embrechts, C. Klüppelberg, T. Mikosch, *Modelling Extremal Events for Insurance and Finance*, Springer, Berlin, 1997. ISBN: 978-3-540-60931-5.

[3] R.W. Katz, M.B. Parlange, P. Naveau, Statistics of extremes in hydrology, *Advances in Water Resources*, Vol. 25, No. 8–12, 2002, pp. 1287–1304. http://doi.org/10.1016/S0309-1708(02)00056-8.

[4] C. G. Anghel, C. Ilinca, Evaluation of Various Generalized Pareto Probability Distributions for Flood Frequency Analysis, *Water*, Vol. 15, 2023, 1557. https://doi.org/10.3390/w15081557.

[5] X. Zhang, L.A. Vincent, W.D. Hogg, A. Niitsoo, Temperature and Precipitation Trends in Canada during the 20th Century, *Atmosphere-Ocean*, Vol. 35, 2000, pp. 395-429. https://doi.org/10.1080/07055900.2000.9649654.

[6] P. de Zea Bermudez, S. Kotz, Parameter estimation of the generalized Pareto distribution Part I, *Journal of Statistical Planning and Inference,* Vol. 140, No. 6, 2010, pp. 1353–1373. https://doi.org/10.1016/j.jspi.2008.11.019.

[7] J. Pickands, Statistical inference using extreme order statistics, *Annals of Statistics*, Vol. 3, No. 1, 1975, pp. 119–131. http://doi.org/10.1214/aos/1176343003.

[8] A.C. Davison, R.L. Smith, Models for exceedances over high thresholds, *Journal of the Royal Statistical Society: Series B (Methodological)*, Vol. 52, No. 3, 1990, pp. 393–442.https://doi.org/10.1111/j.2517-6161.1990.tb01796.x.

[9] L. Fawcett, D. Walshaw, Improved estimation for temporally clustered extremes, *Environmetrics*, Vol. 18, No. 2, 2007, pp. 173–188. http://doi.org/10.1002/env.810.

[10] J. Jonathan, K. Ewans, Statistical modelling of extreme ocean environments for marine design: A review, *Ocean Engineering*, Vol. 62, 2013, pp. 91–109. http://doi.org/10.1016/j.oceaneng.2013.01.004.

[11] S. Beguería, Uncertainties in partial duration series modelling of extremes related to the choice of the threshold value, *Journal of Hydrology*, Vol. 303, No. 1–4, 2005, pp. 215–230. http://doi.org/10.1016/j.jhydrol.2004.07.015.

[12] M.R. Malik, D. Kumar, Generalized Pareto Distribution Based on Generalized Order Statistics and Associated Inference, *Statistics in Transition New Series*, Vol. 20, No. 3, 2019, pp. 57–79. http://doi.org/10.21307/stattrans-2019-024.

[13] J. Martín, M.I. Parra, M.M. Pizarro, E.L. Sanjuán, Baseline Methods for the Parameter Estimation of the Generalized Pareto

Distribution, *Entropy*, Vol. 24, No. 2, 2022, pp. 178. http://doi.org/10.3390/e24020178.

[14] K. Kopczewska, L-moments skewness and kurtosis as measures of regional convergence and cohesion, *Statistica Neerlandica*, Vol. 68, No. 2, 2014, pp. 215–233. http://doi.org/10.1111/stan.12031.

[15] D. Bílková, L-moments and TL-moments as an alternative tool of statistical data analysis, *Journal of Applied Mathematics and Physics*, Vol. 2014, No. 2014, pp. 919-929. http://dx.doi.org/10.4236/jamp.2014.210104.

[16] E.S. Martins, J.R. Stedinger, Generalized maximum-likelihood Pareto–Poisson estimators for partial duration series, *Journal of Hydrology*, Vol. 248, No. 3–4, 2001, pp. 245–265. http://doi.org//10.1029/2001WR000367.

[17] S. El Adlouni, T.B.M.J. Ouarda, X. Zhang, R. Roy, B. Bobée, Generalized maximum likelihood estimators for the nonstationary generalized extreme value model, *Water Resources Research*, Vol. 43, 2007, W03410 http://doi.org/10.1029/2005WR004545.

[18] T. Phoophiwfa, P. Chomphuwiset, T. Prahadchai, J.-S. Park, A. Apichottanakul, W. Theppang, P. Busababodhin, Employing the Generalized Pareto Distribution to Analyze Extreme Rainfall Events on Consecutive Rainy Days in Thailand's Chi Watershed: Implications for Flood Management, *Hydrology and Earth System Sciences*, Vol. 28, No. 2, 2024, pp. 801–816. http://doi.org/10.5194/hess-28-801-2024.

[19] R. Mínguez, Automatic Threshold Selection for Generalized Pareto and Pareto–Poisson Distributions in Rainfall Analysis: A Case Study Using the NOAA NCDC Daily Rainfall Database, *Atmosphere*, Vol. 16, No. 1, 2025, 61. http://doi.org/10.3390/atmos16010061.

[20] R.I. Jennrich, P.F. Sampson, Newton–Raphson and Related Algorithms for Maximum Likelihood Variance Component Estimation, *Technometrics*, Vol. 18, No. 1, 1976, pp. 70–79. http://doi.org/10.1080/00401706.1976.10489395.

[21] R.I. Jennrich, S.M. Robinson, A Newton–Raphson Algorithm for Maximum Likelihood Factor Analysis, *Psychometrika*, Vol. 34, No. 1, 1969, pp. 111–123. http://doi.org/10.1007/BF02290176.

[22] J. Kiefer, J. Wolfowitz, Consistency of the Maximum Likelihood Estimator in the Presence of Infinitely Many Incidental Parameters, *The Annals of Mathematical Statistics*, Vol. 27, No. 4, 1956, pp. 887–906. http://doi.org/10.1214/aoms/1177728066.

[23] E.S. Martins, J.R. Stedinger, Generalized Maximum Likelihood GEV Quantile Estimators for Hydrologic Data, *Water Resources Research*, Vol. 36, No. 3, 2000, pp. 737–744. http://doi.org/10.1029/1999WR900330.

[24] M. Plummer, Simulation-Based Bayesian Analysis, Annual Review of Statistics and Its Application, Vol. 10, 2023, pp. 1–22. http://doi.org/10.1146/annurev-statistics-122121-040905.

[25] C.P. Robert, G. Casella, *Monte Carlo Statistical Methods,* 2nd ed., Springer Texts in Statistics, New York, 2004. ISBN: 978-0-387-21239-5.

[26] R.V. Craiu, P. Gustafson, J.S. Rosenthal, Reflections on Bayesian inference and Markov chain Monte Carlo, *Canadian Journal of Statistics*, Vol. 50, No. 4, 2022, pp. 1-15. http://doi.org/10.1002/cjs.11707.

[27] K. Choi, A review of the Bayesian approach with the MCMC and the HMC as a competitor of classical likelihood statistics for pharmacometricians, *Translational and Clinical Pharmacology*, Vol. 31, No. 2, 2023, pp. 69–84. http://doi.org/10.12793/tcp.2023.31.e9.

[28] J. R. M. Hosking, L-Moments: Analysis and Estimation of Distributions Using Linear Combinations of Order Statistics, *Journal of the Royal Statistical Society: Series B (Methodological),* Vol. 52, No. 1, 1990, pp. 105-124. http://doi.org/10.1111/j.2517-6161.1990.tb01775.x.

[29] J. R. M. Hosking, J. R. Wallis, Parameter and quantile estimation for the generalized Pareto distribution, *Technometrics*, Vol. 29, No. 3, 1987, pp. 339–349. http://doi.org/10.1080/00401706.1987.10488243.

[30] A. Sankarasubramanian, K. Srinivasan, Investigation and Comparison of Sampling Properties of L-Moments and Conventional Moments, *Journal of Hydrology*, Vol. 218, 1999, pp. 13-34. http://doi.org/10.1016/S0022-1694(99)00018-9.

APPENDIX

Table 2. The mean and MSE for parameter estimation in the case of $\mu = 2, \sigma = 2, \xi = 0$.

	Methods	Parameter		MSE	
		Scale (σ)	Shape (ξ)	Scale (σ)	Shape (ξ)
300	ML	2.2329	-0.1105	0.5135	0.0744
	GML	2.2043	-0.1077	<u>0.2563</u>	<u>0.0257</u>
	Bayesian	2.0815	0.1220	0.3810	0.1013
	L-Moments	2.0445	-0.0287	0.3264	0.0506
500	ML	2.1020	-0.0518	0.2241	0.0317
	GML	2.1796	-0.0920	<u>0.1433</u>	<u>0.0122</u>
	Bayesian	2.0172	0.0761	0.1930	0.0397
	L-Moments	1.9912	-0.0002	0.1890	0.0271
700	ML	2.0943	-0.0496	0.1511	0.0214
	GML	2.1733	-0.0896	<u>0.1072</u>	<u>0.0106</u>
	Bayesian	2.0373	0.0356	0.1354	0.0220
	L-Moments	2.0220	-0.0147	0.1412	0.0190
1000	ML	2.0574	-0.0262	0.0945	0.0136
	GML	2.1551	-0.0735	<u>0.0815</u>	<u>0.0087</u>
	Bayesian	2.0181	0.0315	0.0861	0.0147
	L-Moments	2.0018	0.0006	0.0956	0.0143

Source: created by theauthors.

Contribution of Individual Authors to the Creation of a Scientific Article

- Autcha Araveeporn: Conceptualized the study, designed the methodology, performed statistical modeling, wrote the initial draft of the manuscript, and contributed to interpreting the results. Additionally, supervised the research process and coordinated revisions based on reviewer feedback.
- Paradorn Sukpan: Conducted data collection, performed simulations, assisted with statistical analyses.
- Kanchana Kumnungkit: Supported manuscript editing and formatting to meet journal requirements.

Sources of Funding for Research Presented in a Scientific Article or Scientific Article Itself
No funding was received for conducting this study.

Conflict of Interest
The authors have no conflicts of interest to declare that are relevant to the content of this article.